2016

Analysis on Lubricant Film Force for Two Types of Meshing Pair Profile in Single Screw Compressor

Feilong Liu
School of Energy and Power Engineering, Xi'an Jiaotong University, Xi'an, China, China / Department of Flow, Heat, and Combustion Mechanics, Ghent University, Ghent, Belgium, liufeilong@stu.xjtu.edu.cn

Jia Xie
School of Energy and Power Engineering, Xi'an Jiaotong University, Xi'an, China, jiajiawa_1990@163.com

Davide Ziviani
Department of Flow, Heat, and Combustion Mechanics, Ghent University, Ghent, Belgium, davide.ziviani@ugent.be

Quanke Feng
School of Energy and Power Engineering, Xi'an Jiaotong University, Xi'an, China, qkfeng@mail.xjtu.edu.cn

Martijn van den Broek
Department of Flow, Heat, and Combustion Mechanics, Ghent University, Ghent, Belgium, Martijn.vandenBroek@UGent.be

See next page for additional authors

Analysis on Lubricant Film Force for Two Types of Meshing Pair Profile in Single Screw Compressor

Feilong Liu [1], Jia Xie[2], Davide Ziviani[3], Quanke Feng[4]* , Martijn Van Den Broek[5], Michel De Paepe[6]

[1]School of Energy and Power Engineering, Xi'an Jiaotong University,
Xi'an, Shaanxi, China
[1]Department of Flow, Heat, and Combustion Mechanics, Ghent University,
Ghent, Belgium
liufeilong@stu.xjtu.edu.cn
[2]School of Energy and Power Engineering, Xi'an Jiaotong University,
Xi'an, Shaanxi, China
jiajiawa_1990@163.com
[3]Department of Flow, Heat, and Combustion Mechanics, Ghent University,
Ghent, Belgium
Davide.Ziviani@UGent.be
[4]School of Energy and Power Engineering, Xi'an Jiaotong University,
Xi'an, Shaanxi, China
qkfeng@mail.xjtu.edu.cn, Tel(Fax): +86-29-82663783
[5]Department of Flow, Heat, and Combustion Mechanics, Ghent University,
Ghent, Belgium
Martijn.vandenBroek@UGent.be
[6]Department of Flow, Heat, and Combustion Mechanics, Ghent University,
Ghent, Belgium
Michel.DePaepe@UGent.be
* Corresponding Author

ABSTRACT

Single screw compressors are widely used in various industrial fields, however the performance usually drops obviously after thousands of hours of operation due to the wear between the star-wheel and the gate rotor. A lot of meshing pair profiles and manufacturing methods are proposed to solve this problem. Thus, good oil lubrication conditions are conducive to improve the wear resistance of the meshing pair so as to increase the compressor's operation life. In this paper, the geometric models of the clearances for both profiles, a kind of multi-column profile and single-column profile for oil flooded compressors are carried out, and a mathematical lubrication model is used to analyses the oil lubrication. Results show that the torques caused by the oil film force on both sides of the star-wheel tooth are unbalanced. The total torques of the analyzed multi-column profile is smaller than that of the single column profile, which indicates a better lubrication condition. The analysis can also be used to optimize the profile design of the meshing pair of single screw compressors.

1. INTRODUCTION

Since Zimmern (1972) first developed the single screw compressor (SSC) with the profile of straight-line envelope type, it is now widely used in various fields, such as air compression, refrigeration, industrial progress, heat pump and etc.. However, due to the poor wear-resistance performance, the discharge capacity decreases sharply after thousands hours' operation. This is mainly because of the rapid wear of the star-wheel tooth flank surface while meshing with the screw groove, which can extends the clearance and then results in the leakage. A lot of works have been done by Zimmern (1976), Jing (1986), Boblitt (1987), Jensen (2000), Wu et al. (2009) in order to find a suitable structure profile for prolonging the operation life of the meshing pair, including both profile design and manufacturing methods. Feng et al. (2005) also proposed a multistraight-line envelope profile. Then, on the basis of

column envelope meshing pair (CEMP) and multistraight-line envelope profile, a multicolumn envelope meshing pair (MEMP) was developed by Wu et al. (2009) aimed to reduce the friction.

According to Cameron's study (1983), a well formed hydrodynamic lubrication between two sliding surfaces can generate a lubricant film and avoid the wear. Similarly to the meshing pair in SSC, a good lubrication between the screw groove and the tooth flank surface can also reduce or even avoid the wear problem. In the study of Post and Zwaans (1986) about the hydrodynamic lubrication, the tooth will move to the smaller force side because of the unbalanced lubricant film forces generated on each side of the tooth flank. This will lead to the clearances' increasing on one side and decreasing on the other side. According to the research of Jisheng et al. (1997), Huang et al. (2007), Kim et al. (2014) and Larsson (2009), when the change reaches to the critical point, the flow regime will change form hydrodynamic lubrication to boundary lubrication, which will cause the metal contact between the meshing pair and lead to the wear out of the tooth flank. Thus, it is necessary to analyze the lubrication situation between the meshing pair. Huang et al. (2015) created a useful optimization method of the meshing pair profile based on the proposed lubrication simulation analysis about the CEMP.

In this paper, a simulation model is used to analyses the oil lubrication in two types of meshing pair, a kind of multi-column profile and single column profile for oil flooded compressors. Real design parameters of these two types meshing pair for the same single screw compressor are given as calculation examples. The oil lubrication analysis results are then compared and discussed.

2. GEOMETRY MODEL

2.1 Geometric And Kinematic Relations Between The Meshing Pair

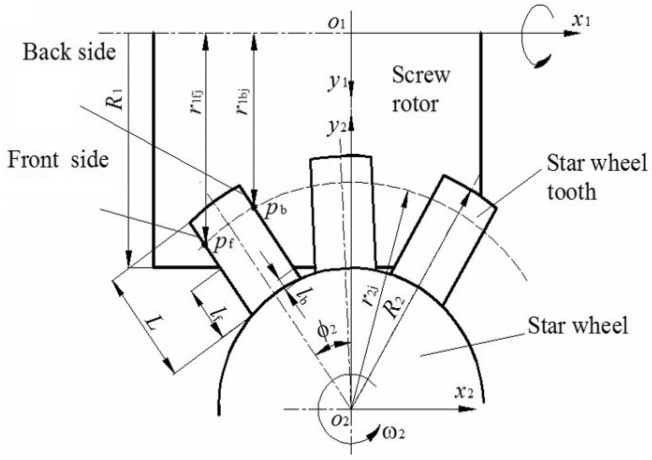

Figure 1: Geometric relations between the meshing pair

Fig.1 shows the relationships between screw rotor and star-wheel while operation. ϕ_2 is the rotation angle. R1 is the radius of the screw rotor. For any contact points P_f and P_b on each side along the tooth, the related swinging radius r_{2j} is

$$r_{2j} = \sqrt{\left(\sqrt{R_2^2 - (b/2)^2} - (L-l)\right)^2 + (b/2)^2} \tag{1}$$

Where R_2 is the radius of the star-wheel, b is the tooth width, l is the distance from the tooth root to the contact point, L is the tooth length.

The swinging radius from the contact point to the rotor center, r_{1fj} and r_{1bj} are

$$\begin{cases} r_{1fj} = a - r_{2j}\cos(\phi_2 + \delta) \\ r_{1bj} = a - r_{2j}\cos(\phi_2 - \delta) \end{cases} \tag{2}$$

Where a is the center distance between the screw rotor and the star-wheel, δ is the space width half angle

$$\delta = \arccos(\frac{b}{2R_2}) \tag{3}$$

The unengaged length on both sides of the tooth l_f and l_b are

$$\begin{cases} l_f = L - \dfrac{R_2 \cdot \cos(\delta + \phi_2) - a + R_1}{\cos\phi_2} \\ l_b = L - \dfrac{R_2 \cdot \cos(\delta - \phi_2) - a + R_1}{\cos\phi_2} \end{cases} \tag{4}$$

2.2 Double-column Meshing Pair

The double-column meshing pair profile is established mainly based on the MEMP, shown in Fig.2. The geometric and kinematic relations between the tooth and the groove can be described by three coordinates. Coordinate, *S (t,n)* is used to describe the center coordinates of the designed columns, which could be given through the design process. The other two Cartesian coordinates S_f (x_f,h_f) and S_b (x_b,h_b) are used for expressing the geometry of the clearances in both sides (front and back) of the tooth. Axes x_f and x_b coincide with the front and back screw groove flank, h_f and h_b two orthogonal axes to x_f and x_b, respectively, which can express the clearances between the screw groove and the tooth flank. As shown in Fig.2, the tooth flanks of the double-column profile are consisted of two column segments and three tangent lines for each side. Points 1-8 are the tangent points of the arcs and lines. The groove inclined angles (α_{f1}, α_{b1}), equals to the inclined angles of the tangent lines at the meshing points (c,d). These angles can be obtained by the geometric and kinematic relations between the star wheel and the screw shown in Fig.1.

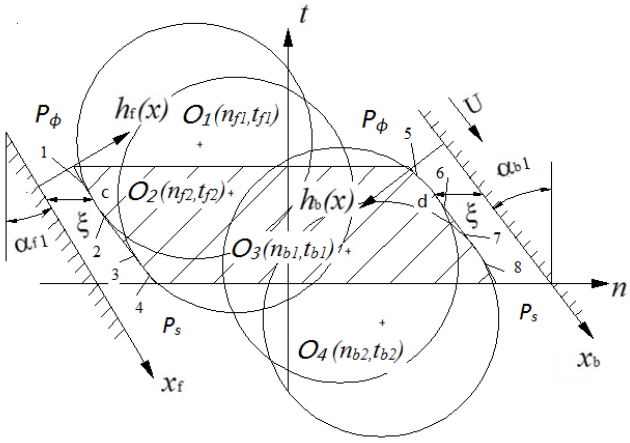

Figure 2: Double-column meshing pair

For this double-column meshing pair profile, columns O_2 and O_3 are the basic columns, which are parallel to the tooth center line. O_1 and O_4 are the auxiliary columns with inclined angles β_f and β_b. According to the MEMP theory proposed by Wu et al. (2009), the center coordinates of the auxiliary columns at any position along the tooth can be calculated once β_f, β_b and the center coordinates on the tooth top are given after design.

The groove inclined angles are expressed as

$$\begin{cases} \tan\alpha_{f1} = \dfrac{\omega_2 r_{2j}}{\omega_1 r_{1fj}} \\ \tan\alpha_{b1} = \dfrac{\omega_2 r_{2j}}{\omega_1 r_{1bj}} \end{cases} \tag{5}$$

The clearance functions for the front side of the tooth can be expressed as follows:

$$h_f(t) = \begin{cases} h_f(t_1) + \dfrac{(t-t_1)\sin(\alpha_{f1}-\alpha_1)}{\cos(\alpha_1)} & t_1 < t \le u \\ \xi\cos(\alpha_{f1}) + r - r\cos(\alpha_{f1} - \arcsin(\dfrac{t_{f1}-t}{r})) & t_2 \le t \le t_1 \\ h_f(t_2) + \dfrac{(t_2-t)\sin(\alpha_2-\alpha_{f1})}{\cos(\alpha_2)} & t_3 \le t < t_2 \\ h_f(t_3) + \dfrac{(t_3-t)\sin(\dfrac{\arcsin(\frac{t_{f2}-t}{r})+\alpha_2}{2} - \alpha_{f1})}{\cos(\dfrac{\arcsin(\frac{t_{f2}-t}{r})+\alpha_2}{2})} & t_4 \le t < t_3 \\ h_f(t_4) + \dfrac{(t_4-t)\sin(\alpha_4-\alpha_{f1})}{\cos(\alpha_4)} & 0 \le t < t_4 \end{cases} \tag{6}$$

$$x(t) = \begin{cases} \dfrac{(u-t)\cos(\alpha_{f1}-\alpha_1)}{\cos(\alpha_1)} & t_1 \le t \le u \\ x(t_1) + \dfrac{(t_1-t)\cos(\alpha_{f1} - \dfrac{\arcsin(\frac{t_{f1}-t}{r})+\alpha_1}{2})}{\cos(\dfrac{\arcsin(\frac{t_{f1}-t}{r})+\alpha_1}{2})} & t_c \le t < t_1 \\ x(t_c) + \dfrac{(t_c-t)\cos(\dfrac{\arcsin(\frac{t_{f1}-t}{r})-\alpha_{f1}}{2})}{\cos(\dfrac{\arcsin(\frac{t_{f1}-t}{r})+\alpha_{f1}}{2})} & t_2 \le t < t_c \\ x(t_2) + \dfrac{(t_2-t)\cos(\alpha_2-\alpha_{f1})}{\cos(\alpha_2)} & t_3 \le t < t_2 \\ x(t_3) + \dfrac{(t_3-t)\cos(\dfrac{\arcsin(\frac{t_{f2}-t}{r})+\alpha_2}{2} - \alpha_{f1})}{\cos(\dfrac{\arcsin(\frac{t_{f2}-t}{r})+\alpha_2}{2})} & t_4 \le t < t_3 \\ x(t_4) + \dfrac{(t_4-t)\cos(\alpha_4-\alpha_{f1})}{\cos(\alpha_4)} & 0 \le t < t_4 \end{cases} \tag{7}$$

Where r is the radius of the designed columns, ξ is the design clearance, u is the thickness of the tooth, α_1 and α_4 are angles of the tangent lines when points 1 and 4 act as the meshing points, which can be got as follows,

$$\begin{cases} \tan\alpha_1 = \dfrac{\omega_2 r_{2j}}{\omega_1 R_1} \\ \tan\alpha_4 = \dfrac{\omega_2 r_{2j}}{\omega_1 (a - r_{2j})} \end{cases} \tag{8}$$

Line 34 is the common tangent line of the two columns whose angle can be calculated according to the geometric relationships between the columns, therefore, $\alpha_2=\alpha_3$. t_1~t_4 are the related height of the points.

$$\begin{cases} t_i = t_{f1} - r\sin(\alpha_i) & i = 1,2 \\ t_i = t_{f2} - r\sin(\alpha_i) & i = 3,4 \end{cases} \tag{9}$$

Similarly to the front side, the clearance functions of the back side can be obtained as well.

2.3 Single-column Meshing Pair

The single-column meshing pair is introduced and studied by Wu and Feng (2009), shown in Fig.3.

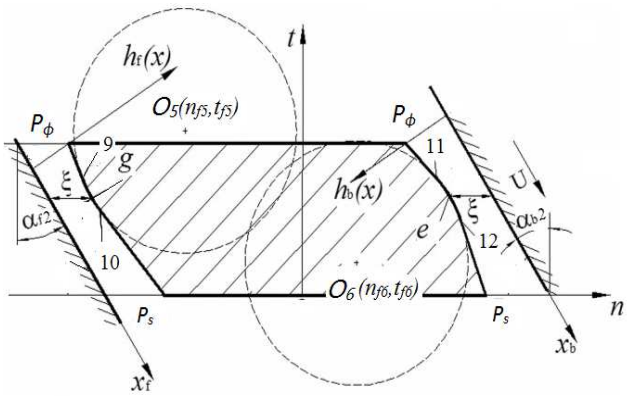

Figure 3: Single-column meshing pair

Three coordinates are also set similarly to the double-column meshing pair to describe the clearances between the crew groove and the tooth flank. The tooth flanks of the single-column profile are consisted of one column segments and two tangent lines for each side. Points 9-12 are the tangent points of the arcs and lines. The groove inclined angles (α_{f2}, α_{b2}), which are related to the meshing points (g,e), can be calculated by

$$\begin{cases} \tan\alpha_{f2} = \dfrac{\omega_2 r_{2j}}{\omega_1 r_{2fj}} \\ \tan\alpha_{b2} = \dfrac{\omega_2 r_{2j}}{\omega_1 r_{2bj}} \end{cases} \tag{10}$$

Then the clearance functions for the front side are

$$h_f(t) = \begin{cases} h_f(t_9) + \dfrac{(t - t_9)\sin(\alpha_{f2} - \alpha_9)}{\cos(\alpha_9)} & t_9 < t \le u \\ \xi\cos(\alpha_{f2}) + r - r\cos(\alpha_{f2} - \arcsin(\dfrac{t_{f5} - t}{r})) & t_{10} \le t \le t_9 \\ h_f(t_{10}) + \dfrac{(t_{10} - t)\sin(\alpha_{10} - \alpha_{f2})}{\cos(\alpha_{10})} & 0 \le t < t_{10} \end{cases} \tag{11}$$

$$x_f(t)=\begin{cases}\dfrac{(u-t)\cos(\alpha_{f2}-\alpha_9)}{\cos(\alpha_9)} & t_9\le t\le u\\ x_f(t_9)+\dfrac{(t_{10}-t)\cos(\alpha_{f2}-\dfrac{\arcsin(\frac{t_{f5}-t}{r})+\alpha_9}{2})}{\cos(\dfrac{\arcsin(\frac{t_{f5}-t}{r})+\alpha_9}{2})} & t_g\le t<t_9\\ x_f(t_g)+\dfrac{(t_g-t)\cos(\alpha_{f2}-\dfrac{\arcsin(\frac{t_{f5}-t}{r})-\alpha_{f2}}{2})}{\cos(\dfrac{\arcsin(\frac{t_{f5}-t}{r})+\alpha_{f2}}{2})} & t_{10}\le t< t_g\\ x_f(t_{10})+\dfrac{(t_{10}-t)\cos(\alpha_{10}-\alpha_{f2})}{\cos(\alpha_{10})} & 0\le t< t_{10}\end{cases} \tag{12}$$

Where α_9, α_{10} are the angles of the tangent lines when points 9 and 10 act as the meshing points, which can be got by:

$$\begin{cases}\tan\alpha_9=\dfrac{\omega_2 r_{2j}}{\omega_1 R_1}\\ \tan\alpha_{10}=\dfrac{\omega_2 r_{2j}}{\omega_1(a-r_{2j})}\end{cases} \tag{13}$$

t_9 and t_{10} are the related height of the meshing points

$$t_i=t_{f5}-r\sin(\alpha_i)\quad i=9,10 \tag{14}$$

The clearance functions for the back side can also be obtained through the same way.

2.4 Lubrication Model

The whole path between the groove and the tooth flank can be divided into two parts by the meshing point, convergent region at the high pressure side, and divergent region at the low pressure side. For the divergent region, the pressure applied on the tooth flank can be seen as the suction pressure.

For the convergent region, the lubrication model introduced by Launder and Leschziner (1978) can be simplified as:

$$\frac{\mathrm{d}P(x)}{\mathrm{d}x}=\frac{6\mu U}{h(x)^2}-\frac{12\mu M}{\rho h(x)^3}+\frac{1.2M^2}{\rho h(x)^3}\cdot\frac{\mathrm{d}h(x)}{\mathrm{d}x}-\frac{0.133\rho U^2}{h(x)}\cdot\frac{\mathrm{d}h(x)}{\mathrm{d}x} \tag{15}$$

Where ρ is the density of the lubrication oil, $h(x)$ is the geometric model of the clearance.

The boundary condition is

$$\begin{cases}x=x_0, P(x)=P_\phi\\ x=x_n, P(x)=P_s\end{cases} \tag{16}$$

Where P_ϕ is the gas pressure in the compressing chamber, P_s is the suction pressure. The pressure distribution along the tooth surface in the convergent region is

$$P(x)=P_{\phi}+\int_{x_0}^{x}\frac{6\mu U}{h(x)^2}\mathrm{d}x-\frac{12\mu M}{\rho}\int_{x_0}^{x}\frac{1}{h(x)^3}\mathrm{d}x \\ -\frac{1.2M^2}{2\rho}\left(\frac{1}{h(x)^2}-\frac{1}{h(x_0)^3}\right)-0.133\rho U^2[\ln h(x)-\ln h(x_0)] \tag{17}$$

Where

$$M=\frac{\frac{12\mu}{\rho}\int_{x_0}^{x_n}\frac{1}{h(x)^3}\mathrm{dt}\text{-}\sqrt{\left(\frac{12\mu}{\rho}\int_{x_0}^{x_n}\frac{1}{h(x)^3}\mathrm{dt}\right)^2+\frac{2\cdot 1.2}{\rho}\left(\frac{1}{h(x_n)^2}-\frac{1}{h(x_0)^2}\right)N}}{\frac{1.2}{\rho}\left(\frac{1}{h(x_0)^2}-\frac{1}{h(x_n)^2}\right)} \tag{18}$$

$$N=\int_{x_0}^{x_n}\frac{6\mu U}{h(x)^2}\mathrm{d}x\text{-}0.133\rho U^2[\ln h(x_n)-\ln h(x_0)]+P_s-P_{\phi} \tag{19}$$

U is the relative velocity between the meshing pair

$$U=\sqrt{(\omega_2 r_{2j})^2+(\omega_1 r_{1(f,b)j})^2} \tag{20}$$

Then, the component forces caused by the oil film and the gas force, applied on the engaged element dl, which are parallel to the upper surface of the star-wheel are

$$\begin{cases} F_{oij}'=\cos\alpha\cdot\int_{x_0}^{x_n}P(x)dx \\ F_{gi}=\cos\alpha\cdot\int_{x_n}^{x_s}P_s dx \end{cases} \tag{21}$$

Where α is the groove inclined angle of the related meshing point.

The gas force, applied on the unengaged element *dl*, which is parallel to the upper surface of the star-wheel is

$$F_{gi}'=u\cdot P_s \tag{22}$$

Therefore, the torques applied on each side of the tooth are

$$\begin{cases} T_{fi}=\int_{l_f}^{L}F_{foij}'\cdot r_{2j}(l)dl+\int_{l_f}^{L}F_{fgi}\cdot r_{2j}(l)dl+\int_{0}^{l_f}F_{fgi}'\cdot r_{2j}(l)dl \\ T_{bi}=\int_{l_b}^{L}F_{oijb}'\cdot r_{2j}(l)dl+\int_{l_b}^{L}F_{bgi}\cdot r_{2j}(l)dl+\int_{0}^{l_b}F_{bgi}'\cdot r_{2j}(l)dl \end{cases} \tag{23}$$

Where l_f, l_b and $r_{2j}(l)$ can be got through equation (2~4).

The composite torque applied on one tooth is as follows：

$$T_i=T_{bi}\text{-}T_{fi} \tag{24}$$

During operation, there are usually three or four star-wheel teeth participating in the engaging at the same time. Thus, the total torque applied on the star-wheel is

$$T=\sum_{1}^{4}T_i \tag{25}$$

3. RESULTS

In this paper, two different designs of the two profiles for the same 2 m³/min oil-flooded single screw air compressor are taken as calculation examples. The Dimensions of the single screw compressor is shown in Tab. 1.

Table 1: Dimensions of the single screw compressor

Main Parameter	Value	Main Parameter	Value
Screw rotor radius R_1/*mm*	65	Tooth length *L/mm*	30
Star-wheel radius R_2/*mm*	61	Center distance *a/mm*	96
Tooth width *b/mm*	18	Envelope column radius *r/mm*	6
Rotating speed / $r{\cdot}min^{-1}$	2970	Discharge pressure $P_{out}/10^5 Pa$	10
Design clearance ξ/*mm*	0.04		

Table 2: Design parameters

Parameter	*n/mm*	*t /mm*
Tooth top of Column O_1	-4.754	7.292
Column O_2	-2.674	4.542
Column O_3	2.674	0.958
Tooth top of Column O_4	4.739	-1.792
Column O_5	-2.674	4.542
Column O_6	2.674	0.958

Tab. 2 is the design parameters related to the two different profiles. For the double-column, β_f=2.327°, β_b=-2.298°.

Fig.4 is the pressure distributions of the two types meshing pair under the discharge starting rotation angle (ϕ_2=35°) at the tooth top.

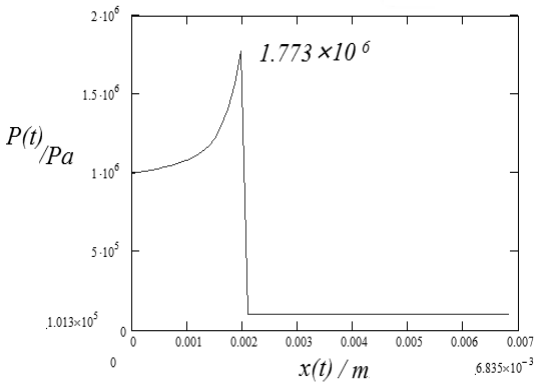

(a) Pressure distribution for double-column meshing pair

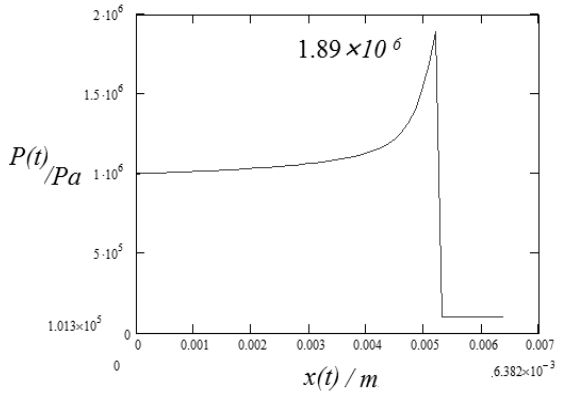

(b) Pressure distribution for single-column meshing pair

Figure 4: Pressure distributions at the top tooth

In both types of the meshing pair, the pressures increase in the convergent region, and will reach the peak value at the meshing point. For the double-column meshing pair, the peak pressure is 1.773×10^6 Pa. For single-column meshing pair, the peak pressure is 1.89×10^6 Pa.

The total torques of the two types meshing pair through the rotation angle ϕ_2 are shown in Fig.5. Obviously, the torques for both profiles have periodical changes during the operation. For the double-column, the total torque changes from 1.3 N·m to 3.7 N·m. For the single-column, the total torque changes from 2.92 N·m to 4.5 N·m. At any same rotation angle, the total torque applied on the double-column star-wheel is always smaller than that of the single-column. According to the study of Post and Zwaans (1986), there will be clearance changes between the meshing pair and the single-column meshing pair will have a larger clearance change because of the larger unbalanced torques. From the researches of Jisheng et al. (1997), Huang et al. (2007), Kim et al. (2014) and Larsson (2009), if the change reaches the critical point, the flow regime will change form hydrodynamic lubrication to boundary lubrication, which will cause a metal contact between the meshing pair and lead to the wear out of the tooth flank. That means the double-column have a better lubrication situation.

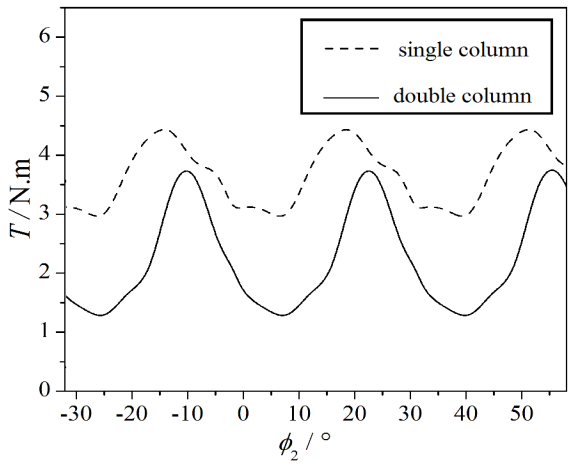

Figure 5: Total torques through the operation

4. CONCLUSIONS

In this paper, a simulation model is used to analyses the oil lubrication in two types of meshing pair. Real design parameters of these two types meshing pair for the same single screw compressor are given as calculation examples. Several conclusions can be made according the calculating results:

- The pressure increases to a peak value from the start of the convergent region to the meshing point.
- The total torques caused by the oil film forces are unbalanced, which would lead to a deflection of the tooth in order to regain balance. Furthering result in changes in the clearances between the meshing pair and may cause metal contact of the meshing pair reducing the operation life.
- The total torque generated by the double-column meshing pair profile is smaller than that of the single-column at any same rotation angle, which indicates the double-column meshing pair profile has a better hydrodynamic lubrication state and a longer operation life.
- The analysis can also be used to optimize the meshing pair profile design for single screw compressors.

REFERENCES

Zimmern, B., and Patel, G. C.(1972) "Design and Operating Characteristics of the Zimmern Single Screw Compressor,"(96–99). Compressor Technology Conference, Purdue

Zimmern B.(1976). Rotary inter-engaging worm and worm wheel with specific tooth shape. US Patent No. 3932077.

Jin GXTY(1986). A study of the single screw compressor profile(312–20). In: Proc. Purdue Compressor Technology Conference.

Boblitt, W.W.(1987). Method for Cutting Complex Tooth Profiles in a Cylindrical, Single-screw Gate-rotor. US Patent No. 4710076.

Jensen, D.(2000). Method for Manufacturing Fluid Compression/Compressor Rotor. US Patent No. 6122824.

Weifeng Wu, Quanke Feng, Column envelope meshing pair and its design method for single screw compressors. J Zhejiang Univ Sci A 2009 10(1):31-36.

Feng Q. K., Guo B., Zhao C., Xu J., Li Y.J., Cheng L., and Shu P.C.,2005, "A Design Method of Meshing Pair Profile of Single Screw Compressors Enveloped by Multi Straight Line," Compressor Technology, 191(3)pp.1–6(in Chinese).

Weifeng Wu, Quanke Feng, 2009, A Multicolumn Envelope Meshing Pair for Single Screw Compressors. ASME J. Mech. Jul., 131, p. 074505.

Cameron A. Basic lubrication theory. Brisbane, Queensland, Australia: Jacaranda-Wiley Ltd: Jacarand Press, 1983, p.17.

Post W and Zwaans M. (1986). Computer simulation of the hydrodynamic lubrication in a single screw compressor(334–348). In: Proceedings of Purdue compressor technology conference, West Lafayette, IN, USA.

Jisheng E and Gawne DT. Influence of lubrication regime on the sliding wear behaviour of an alloy steel. Wear 1997; 211: 1–8.

Huang P, Meng YG and Xu H. Tribology course. Beijing: China Higher Education Press, 2007, p.359.

Kim D-W and Kim K-W. Effects of sliding velocity and ambient temperature on the friction and wear of a boundary-lubricated, multi-layered DLC coating. Wear 2014; 315: 95–102.

Larsson R. Modelling the effect of surface roughness on lubrication in all regimes. Tribol Int 2009; 42: 512–516.

Huang R, Li T, et al. An optimization of the star-wheel profile in a single screw compressor [J]. Proceedings of the Institution of Mechanical Engineers, Part A: Journal of Power and Energy, 2015, 229(2): 139-150.

Lauder BE and Leschziner M. Flow in finite-width, thrust bearings including inertial effects 1-Laminar Flow. ASME J Lubric Technol 1978; 100: 330–338.